Advances in Geosciences
Vol. 17: Planetary Science (2008)
Eds. Namsik Park *et al.*

CHARGED PARTICLE ACCELERATION IN THE HERMEAN MAGNETOSPHERE: THE COMPARISON OF CONTRIBUTIONS OF DIFFERENT MECHANISMS*

ZELENYI LEV
Space Research Institutes RAS
Moscow, 117997, Russia
lzelenyi@cdi.ucla.edu

MALOVA HELMI
Nuclear Physics Institute
Moscow State University, Moscow, Russia

KORZHOV ALEXEY
Moscow Engineering Physics Institute
Moscow, Russia

POPOV VICTOR
Physics Department
Moscow State University, Moscow, Russia

DOMINIQUE DELCOURT
Laboratoire de Physique des Plasma
CNRS, Saint-Maur-des Fosses, France

ARTEMYEV ANTON
Space Research Institutes RAS
Moscow, 117997, Russia

Several important mechanisms of plasma particle acceleration and heating in the Hermean magnetosphere were investigated in a frame of different numerical models. It is shown that the most effective acceleration mechanisms for Mercury are particle scattering on magnetic turbulence in the magnetotail and one of multiple dipolarizations during substorm activity. The comparison with plasma processes in the Earth's magnetosphere demonstrate that the role of these mechanisms is more important near Mercury because of its small magnetosphere and the close distance to the Sun.

*This work is supported by RFBR grants 09-02-00407, 06-02-72561 and HIII 472.2008.2.

1. Introduction

The magnetic field of Mercury, the first planet of the solar system was discovered in 1974 during Mariner-10 flyby near the planet. Due to Mariner-10 mission across the Hermean magnetosphere (the region where the own planetary magnetic field dominate) the first data about the structure and dynamics of the magnetosphere were obtained, that reveal the great interest to investigations of Mercury and its plasma envelope [1]. Now Mariner-10 is not a single spacecraft to study Mercury. The American probe Messenger launched in 2004 towards Mercury, has done two flyby near Mercury the 14 January and the 4 October 2008. The next flight is expected the 29 September 2009 y., after this in March 2011 this spacecraft will go the stationary orbit around the planet to systematic exploration [2]. In 2014 the launch of two Japanese-European spacecraft BEPI Colombo is planned, that reach the orbit of Mercury in 2020 and then become its constant satellites [3].

The measurements of the magnetic fields and particle composition near the planet by Mariner-10 were quite contradictory and provoked many questions, answers for which might be obtained only in the course of new measurements [4], [5]. This problem is very important because of future space missions to Mercury and proposed detailed measurements near it.

To understand what mechanisms of charged particle acceleration might effectively exist in the Hermean magnetosphere, let us remind its essential parameters. The strength of the magnetic field at the planetary surface is 100 times weaker than in the Earth's one. From the site of the Sun the magnetosphere of Mercury is strongly stressed by the solar wind flow, otherwise, from the night side it is strongly elongated and have well expressed tail structure (figure 1). The volume of the Hermean magnetosphere is only 5% from the Earth's one, the magnetopause in the lobe point is situated at the distance only 1.1-1.5 R_M ($R_M \approx 2400$ km) from the center of the planet. Contrary to the Earth the Mercury occupies the larger relative volume of the magnetosphere, this is a reason of its more simple structure with absent both ionosphere and atmosphere, but existing exosphere. Exosphere consists essentially from neutral atoms He, protons, ions Na, K, Ca, Si, and water molecules (discovered recently by spacecraft Messenger), observed in the tail area at distances to 20000 km and more in anti-sun direction. The density of Na^+ ions in the tail, accordingly to Messenger data, is estimated as 10^{-2}-10^{-1} sm^{-3} in the morning and evening sectors [6].

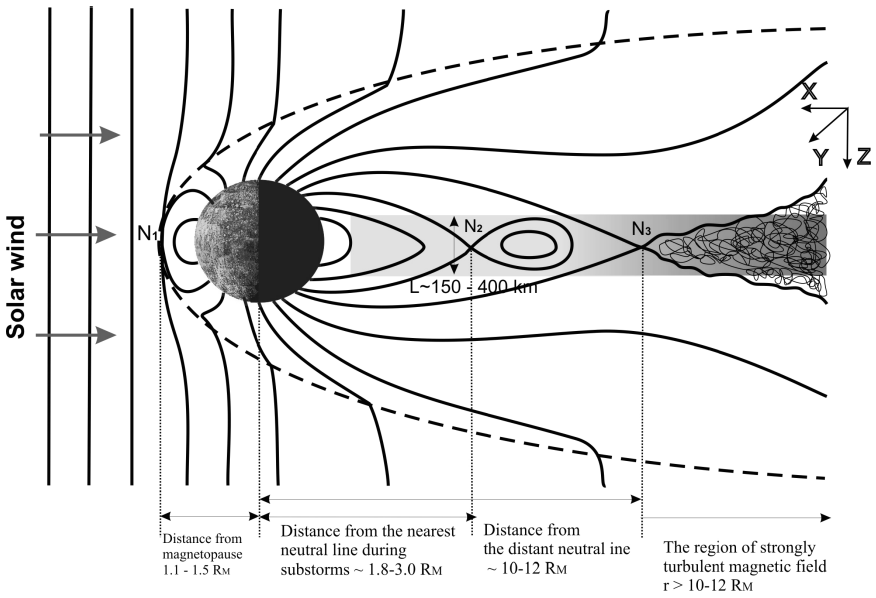

Fig. 1. The scheme of the Hermean magnetosphere is shown with approximate distances of most important magnetospheric regions to the center of the planet. We have chosen the GSM system of reference where Z-axis is directed along the magnetic moment of the planet and X-axis is directed from the center of Mercury in Sun direction. The dashed line shows the position of the magnetopause. Line N1 is the neutral line at the subsolar point magnetopause where the reconnection of magnetic field lines of solar wind and the intrinsic magnetic field of Mercury occurs. At the night side one can see the general structure of the magnetosphere during geomagnetic perturbation when the neutral line N_2 appears near Mercury. The possible thickness of current sheet L is shown. In the area of the distant neutral line N_3 the process of magnetic reconnection is denoted, which is followed by reversed disconnection of magnetic field lines of solar wind from magnetic field lines of the Hermean magnetosphere. Downward from the flow (at the right from the line N_3) the influence of the magnetic field is weakened and there the region of a strong turbulence should exist likely the Earth's one.

Accordingly the principle of similarity based on the topological resemblance of the Earth's and Hermean magnetospheres [7], [8], [9], the scale of space processes in the last one is about 1:8 from the Earth's ones, the scales of temporal processes relatively terrestrial ones are about 1:30. Figure 1, accordingly to the similarity principle demonstrates the approximate scales of the planetary magnetosphere and the mutual position of neutral lines in it. The observations of Mariner-10 demonstrated that the current sheet in the magnetotail is very thin with thickness about several hundreds of kilometers [9]. This signifies that particle motion

in magnetotail might be non-adiabatic [10]. Plasma particles might be demagnetized in current sheet and go with characteristic "serpentine-like" or "meandering" motion from morning to evening sector and might be accelerated by the cross-tail electric field. Due to very small magnetic moment of the planet and the strong flow of falling solar wind, the Hermean magnetosphere is expected to be very dynamical, quickly changing and turbulent [6]. Accordingly to Mariner-10 data, the characteristic scales of temporal changes of Hermean magnetic field are about several minutes [9], the perturbations being followed by appearance of fast and strong flows of energy particles with energies more than 35 keV [11]. These data might testify about the large frequency of substorm perturbations in Mercurian magnetosphere [5], [7] and reconnection processes in the magnetotail [6], [7].

The analysis of experimental data of Mariner-10 the electron flows were discovered with energies up to 300 keV [7], [11] or 600 KeB [5] and protons with energies from 500 keV to 1.9 MeV. The estimate of proton energy from another satellite Helios-2 [12] gives diapason 87 -176 keV. Simultaneous observations of energy protons and electrons in the Hermean magnetosphere provoked many questions. The essential critic was directed against observation of energy protons. Thus, Armstrong *et al.* (1975) supposed that any accelerated protons were present; the simple explanation is the wrong interpretation of measurements of proton detector. Christon *et al.* [13] and later Eraker and Simpson [5] concluded that accelerated electrons obviously are the result of explosive energy release during substorms, whereas the data of proton detector are not clear, therefore the question about accelerated protons is open. Later conclusion by Christon [8] was even more categorical: no accelerated proton flows were registered in the Hermean magnetosphere. The theoretical analysis by Zelenyi *et al.* [14] of particle acceleration by inductive electric field during multiple sporadic reconnections has shown that the upper limit of particle energies can not exceed 50-60 keV. Later this assumption was confirmed by Ip [15] in his model where the ion acceleration during large-scale magnetospheric reconfiguration reached several tens of keV. For comparison, in the Earth's magnetosphere the ion and electron populations might be accelerated to energies about 1 MeV. Messenger flied across the Hermean plasma sheet where plasma density is about $1\,\mathrm{sm}^{-3}$ and had registered the energy particles with energies no less than several hundreds eV [16], also the electrons with energies from 1 to 10 keV were registered. To date, no observation show evidences of hot ions in magnetosphere of Mercury, although in the region of magnetosheath (located between magnetopause

and the bow shock) one expects to see hot Na^+ ions of planetary origin with energies 10-100 keV, that should be accelerated by turbulent electric fields [17].

The aim of this work is the comparison of two essential mechanisms of particle acceleration in the magnetotail of Mercury, based on the models of particle acceleration as a result of multiple dipolarizations and as a result of particle scattering on plasma turbulence. These results are compared with another estimates of the effectiveness of different acceleration mechanisms that might contribute in terrestrial conditions, but (as we propose) can not play essential role in Mercury conditions. Finally in our work we have done a prognosis of possible character of energy spectra of charged particles that are expected to register in future measurements of satellites Messenger and BEPI Colombo.

2. Comparison of Mechanisms of Particle Acceleration in Magnetospheres of the Mercury and the Earth: The Similarity and Difference. Basis of the problem

In the Earth's magnetosphere the essential role in particle acceleration might be played by following mechanisms [18], collected in the Table 1:

1. The acceleration by induction electric fields during substorm dipolarizations [19];
2. The stochastic acceleration of charged particles in turbulent magnetic fields, i.e. Fermi acceleration [20];
3. non-adiabatic acceleration in stationary configurations with minimum of magnetic field in the current sheet of magnetotail by "dawn-dusk" electric field; during reconnection processes near X-lines [14], [21];
4. Plasma particles heating on ULF waves [22], [23];
5. Nonadiabatic heating and acceleration on bow shock and magnetopause [2].

The first acceleration mechanism in terrestrial mechanism has the peculiarity: the interval between storms is from one to several days. During this interval many particles have a time or to escape the Earth's magnetosphere or to move to another regions of magnetosphere (e.g., to be trapped in the dipole magnetic field or to escape from the lobes of magnetosphere through the magnetopause etc), therefore at the next substorm cycle the most part of particle population should be changed.

Table 1. The essential mechanisms of charged particle acceleration and heating in the Earth's magnetosphere. The last two mechanisms are not included in the Table because there are not reliable estimates about their importance in magnetotail observation of accelerated particles.

N	Mechanism	Authors	Gain of energy
1	Acceleration of O^+ by inductive electric fields	Delcourt *et al.* [19]	from several tens eV to more than hundreds keV
2	Stochastic acceleration	Zelenyi *et al.* [41]	up to 30 times relatively the initial energy
3a	Nonadiabatic acceleration	Ashour-Abdalla *et al.*, [30] (and references therein); Delcourt and Martin, [21]	About several tens of keV
3b	Inductive acceleration of p^+ near X-line	Zelenyi *et al.*, [14]	From 1 keV to 1.6 meV

It is shown that for the Earth's magnetosphere the mechanism of plasma acceleration due to single substorm dipolarization is very effective ([24], and references therein). Another situation is in Mercury magnetosphere were, as we mentioned above, the global magnetic perturbations might follow with interval several minutes [15], [19], i.e. one can expect th during several consequent dipolarizations. We suppose that multiple dipolarizations here might be one of the most effective mechanisms of particle acceleration and we present in this article the results of corresponding calculations.

The second mechanism mentioned in the Table 1 plays an important role in the space physics. The pioneerwork in this area belongs to Fermi [25], which proposed that charged particles colliding with chaotically moving obstacles (interstellar and intergalactic clouds) might be accelerated to high energies; this allowed to explain the nature of cosmic rays with ultra-relativistic energies. In th near-Earth region of the magnetosphere where the ordered dipole magnetic field dominates, Fermi acceleration can not play substantial role. At the same time in the distant regions of the Earth's magnetosphere (at distances about or more 100 R_E from the planet) the normal component of the magnetic field B_z (so called residual dipole field) becomes neglectively small, then the role of low-frequency plasma turbulence in particle acceleration might be very effective [20], [26], [27].

Contrary to the Earth, particle acceleration on turbulent electric and magnetic fields of Mercury might take place in magnetotail quite close to the planet. It is due to the small size of magnetic Hermean dipole and to

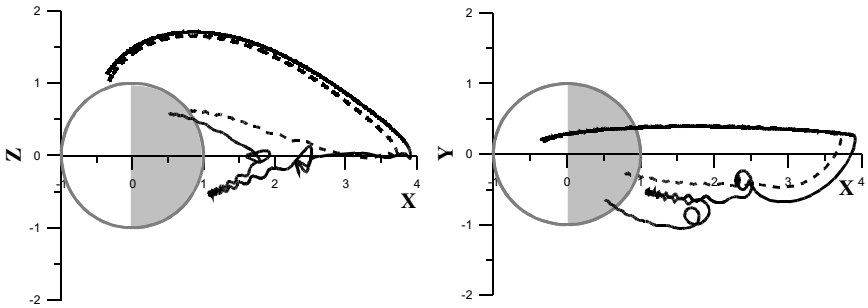

Fig. 2. Two projections of trajectories of two test ions accelerated by convective electric field in the Hermean magnetotail.

powerful dynamical variations of the solar wind flow that influences the Hermean magnetosphere more strongly than the Earth's one. One should expect that the problem of a spatial scale necessary for particle to be accelerated during "chaotic walk" is more important for Mercury having a small and dynamic magnetosphere. In this work we try to estimate the maximum gain of energy for plasma particles due to Fermi acceleration on low-frequency plasma turbulence.

The third mechanism of nonadiabatic acceleration in a neutral sheet of magnetotail shown in Figure 2, plays very important role in the Earth's magnetosphere; there it is quite well investigated [28], [29], [30]. Charged particles are demagnetized near the neutral sheet and go along meandering orbits [10] in the field $B_z(x)$ (here we consider the special solar-magnetospheric system of reference where X axis is directed from the Mercury to anti- Sun direction, Y axis is directed from dawn to dusk), during this motion particles are accelerated by large-scale electric field E_y across the tail. Moving together with convective flow with some average velocity v_d, particles are demagnetized in a neutral plane and return to the planet as it is shown in Fig. 2. Every time when particle cross the neutral sheet, non-adiabatic ions are accelerated by the electric field. Energy gain when particle move along magnetotail (X-direction) is estimated as [31]:

$$W(x) = 2m_i c^2 E_y^2 / B_z^2(x) \tag{1}$$

The comparison of parameters of nonadiabatic proton acceleration in a neutral sheet and corresponding gain of energy for the Earth and Mercury

are presented in Table 2:

Planet	Earth	Mercury
Characteristic energies p^+, keV	0.1–1	0.1
Cross-tail electric field E_y, mV/m	0.1	5
Strength of the magnetic field H, nT	20	40
Potential jump across the magnetotail $\Delta\phi$, keV	Up to 120	from 20 to 50
Characteristic scale across the magnetotail, km	25 $R_E \sim 160000$	4 $R_M \sim 10000$
Gain of energy ΔW, keV	few tens	Up to 10
Relative gain of energy $\Delta W/W_0$	50	10

The electron population regardless small scales of the Hermean magnetosphere should be magnetized therefore the nonadiabatic acceleration is not substantial for it, contrary to protons. The estimate of magnetospheric ion acceleration by inductive electric fields near X-line were done in works by Eraker and Simpson [5] and Baker *et al.* [32], where the possibility of electron acceleration due to reconnection to 100 eV in the Hermean magnetotail is supposed. The theoretical estimate of proton acceleration is done in paper by Zelenyi *et al.* [14]. 1D model of multiple sporadic reconnections of magnetic field $B(t)$is used in the form:

$$B(t) = B_{0x} \tanh(z/L)\vec{e}_x + B_z(t) \sin kx \cdot \vec{e}_z \qquad (2)$$

where $B = B_z(t) = B_{0z}/(1 - t/\tau_r)$; $B_{0z} = B_z(0)$. The last term in expression (2) is the regular part of magnetic field that describes the appearance of magnetic isles during a characteristic time τ_r. It was shown that proton energy gain in the Earth's magnetosphere at the ratio $B_{0z}/B_0 = 0.1$ (B_{0z} and B_0 are, correspondingly, the normal and the total components of the magnetic field) is approximately ≈1.6 MeV. At the same time for the Hermean magnetosphere the energy gain is several times less and it is about ≈50–60 keV. Therefore this mechanism can not be essential in charged particle acceleration and heating in Mercury.

The mechanisms of particle heating at ultra low frequency waves (ULF) and at the bow hock of Mercury (number 4^{th} and 5^{ve} in the Table 2) undoubtedly are interesting for near-Earth investigations. However for the Earth's magnetosphere the acceleration and the scattering of particles due to these mechanisms play the general role near radiation belts. As we have mentioned radiation belts are absent near Mercury. The ULF waves

were observed by Messenger at dayside near the planet [6]. These waves are observed presumably at the dayside of Mercury, therefore they not substantially influence particle acceleration in the Hermean magnetotail.

Therefore, from our point of view, the essential attention in investigations of general mechanisms of acceleration should be paid to ones that were not well studied for Mercury, i.e. the acceleration due to multiple substorm dipolarizations and acceleration on plasma turbulences. To do this we developed and investigated corresponding theoretical methods. Below we present their description.

3. The Model of Charged Particle Acceleration Due to Multiple Substorm Dipolarizations

The modeling of charge particle acceleration in Mercury magnetosphere is actual due to planned satellite missions MESSENGER and Bepi Colombo. The one of the dipolarization characteristic events during magnetospheric substorm is a magnetotail evolution from very elongated state to dipole-like one (Figure 3).

It was shown in 2D model of the Hermean magnetosphere [15] that proton and He^+ acceleration for on cycle of magnetic field dipolarization reached energy about 20 keV. The study of electron acceleration in the adapted for Mercury model T-89 was done in paper by Delcour *et al.*, [19]. It was demonstrated that electrons with initial energies up to several hundreds eV can no be accelerated to energy several keV and more. However, no one of abovementioned models canons not explain high-energy (above hundreds of keV) registered by Mariner-10 (see Introduction).

In paragraph 3.1. we have considered the model of a Hermean magnetosphere analogical to Lui and Rostoker, [33], Luhmann and Friesen,

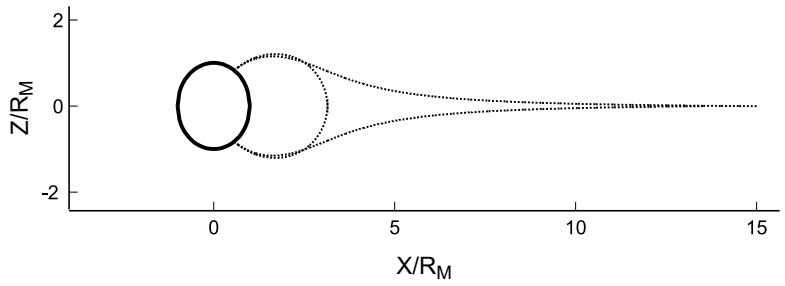

Fig. 3. Scheme of Hermean magnetotail.

[34] model, where electrons and ions might be accelerated due to multiple dipolarizations, where the gain of energy is quite large. Paragraph 3.2. concerns the effects of particle acceleration in magnetic clouds [20], [35].

3.1. *The model of electric and magnetic fields during multiple dipolarization*

Particle tracing is done in the modified Luhmann and Friesen [34] global magnetospheric model of Mercury that is as a superposition of magnetic dipole and Harris current sheet [36]:

$$B_x = \frac{3\mu zx}{r^5} + B_0 \tanh\left(\frac{z}{L}\right), \quad B_y = \frac{3\mu zy}{r^5}, \quad B_z = \mu\frac{2z^2 - x^2 - y^2}{r^5} \quad (3)$$

The changes of magnetic field geometry, i.e. dipolarization, is cyclic. The duration of the dipolarization phase (when the dipole magnetic field dominates) is chosen as $\tau_{m1} = 5\,\mathrm{s}$, one of compression phase (when the magnetotail becomes to be very elongated), is taken as $\tau_{m1} = 25\,\mathrm{s}$.

The characteristic thickness of the magnetosphere $L(t)$ and the electric field E_y in the expansion phase (marked by index "1", $0 \le t \le \tau_{m1}$) and in the compression phase (index "2", $\tau_{m1} \le t \le \tau_{m2}$) are shown in Figure 4.

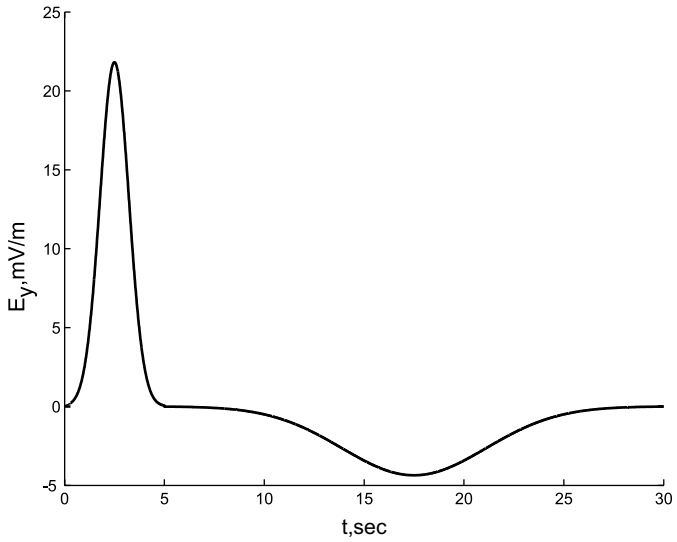

Fig. 4. Electric field as a function of time.

Analogically to work [19] at $\tau_{m1} = 5$ and the amplitude of the electric field about 20 mV/m.

We have estimated the maximum of the gained energy in the expansion phase in dimensional form:

$$W_{ion} \approx \left(\frac{e^2 B_0^2 L_0^2}{m_i c^2} \right) [\ln(2)(\xi - 1)]^2 \tag{4}$$

Here current sheet thickness is $L_0 \leq L \leq \xi L_0$ and parameters L_0, ξ are taken analogically to work [19]. The estimate (4) is correct for the ions with mass m_i and some initial energy, that have not time to escape from the magnetosphere at the time τ_{m1}. For electrons which go across the magnetosphere faster than τ_{m1}, the estimate (4) can not be applied. We obtain the following estimate of electron energy:

$$W_{elect} \approx \frac{32 \ln(2)(\xi - 1) L_0 R_M e B_0}{c\sqrt{\pi}\,\mathrm{erf}(2)} \tag{5}$$

The estimate (5) is correct at $X > 9R_M$.

The values of particle energies, calculated accordingly formulas (4) and (5) and the maximum energies during all modeling cycles are presented in the Table 3. These results lead to conclusion that the mechanism of multiple dipolarizations is effective for heavy exospheric ions. These charged particles, as electrons, as protons having the solar wind as a source are presumably accelerated during the first cycle (it concerns in the first place the electrons).

–	The maximum energy at the first cycle	The maximum of registered energy in the model
e	230 keV	220KeV-1st cycle
p	135 keV	160KeV-2-nd cycle
He^+	34 keV	160KeV-5nd cycle
O^+	9 keV	80KeV-10nd cycle
Na^+	6 keV	62KeV-8th cycle
S^+	4 keV	52KeV-6th cycle
K^+	3.5 keV	45KeV-5th cycle

3.2. *Particle acceleration on "magnetic clouds" in a global model of the Hermean magnetosphere*

Particle acceleration and transport in the Earth's magnetotail depends on the properties of a plasma turbulence generated by ensemble of multiple eigenmodes of magnetotail current sheet. This turbulence might be described, for example, as a set of electric and magnetic waves with arbitrary set of phases and amplitudes in plasma. Another way to investigate a turbulent plasma motion in the magnetotail is the study of particle transport and acceleration on magnetic bubbles, oscillating around some average position. In this paragraph we present the results of particle acceleration in the Hermean magnetosphere with help of the Luhmann and Friesen [34] model, adapted to Mercury by Delcourt *et al.* [19] and modified for our studies in this work. Magnetic perturbation in the form of oscillating bubbles was added in a spatial region at the night side in magnetotail. The contribution of this mechanism of plasma acceleration is compared with acceleration processes in the model of arbitrary propagating wave packets, considered in the next paragraph.

It is supposed that the magnetotail region, limited in {x,y,z} directions ($L_{0x} < x < L_{0x} + \Delta L_x$, $|y| < \Delta L_y$, $|z| < \Delta L_z$), is filled by round 3D magnetic bubbles having for simplicity the single spatial sizes $\lambda = \{\lambda_x, \lambda_y, \lambda_z\}$, where $\lambda_x = \lambda_y = \lambda_z$. The vector potential of the magnetic perturbation of a single i-th bubble ($i = 1, 2 \ldots N$) is taken in the form:

$$\mathbf{A} = \delta \sum_{i=1}^{N} \exp\{-\mathbf{s}^2\}, \quad \mathbf{s} = (\mathbf{r} - \mathbf{r}_{0i} - \mathbf{a}\cos\omega t)/|\boldsymbol{\lambda}| \tag{6}$$

where δ is the normalization coefficient of the vector potential, $x_{0i} = L_{0x} + \Delta L_x \alpha_x$, $y_{0i} = \Delta L_y(2\alpha_y - 1)$ and $z_{0i} = \Delta L_z(2\alpha_z - 1)$ are positions of i-th center of oscillating bubbles, $\boldsymbol{a}$ are amplitudes of spatial bubble oscillations that are chosen equal, $\boldsymbol{\alpha}$ are arbitrary values, homogeneously distributed in the interval $[0, 1]$.

Figure 5 demonstrates 2D distribution of magnetic bubbles in the magnetotail of Mercury, initiated in the box $x_i \in [1, 20]$, $y_i \in [-4, 4]$, $z_i \in [-0.5, 0.5]$. The size of bubbles was taken quite realistic for magnetotail conditions, i.e. about proton gyroradius. The typical trajectory of proton in the planetary magnetotail where the bubble region is extended at $[-0.35, +0.35]$ in Z-direction is shown in Figure 6 in three projections. One can clearly see that in this region its motion is chaotic due to scattering

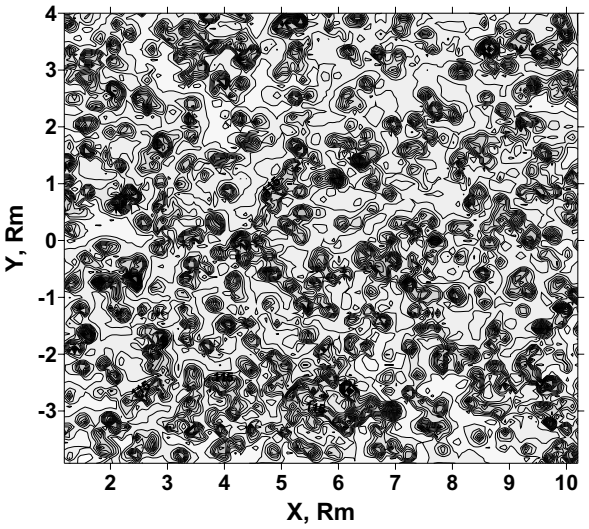

Fig. 5. The distribution of magnetic perturbations in the magnetotail of Mercury.

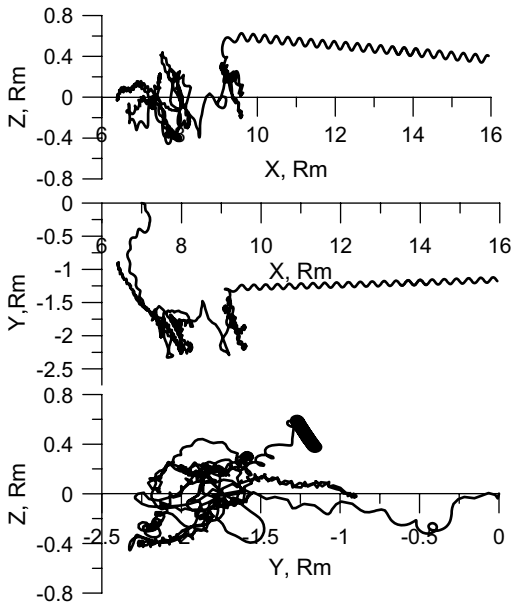

Fig. 6. Three projections of characteristic p^+ trajectory in the presence of magnetic and electric bubbles in magnetotail neutral sheet.

processes. After 80 s of travel proton leaves the region of chaotic scattering, correspondingly the gain of energy is ended.

In a Table 4 we show the results of acceleration of different ion populations that were more frequently registered in the exosphere and magnetosphere of Mercury: H^+, He^+, O^+, Na^+, S^+ and K^+. Initial energies of particles were 500 eV (in some calculations the initial energy 10 eV was tested, but it does not change the final gain of energy on moving bubbles). In each calculation particles were initially distributed homogeneously over the Hermean magnetotail. The results in Table 1 demonstrate the averaged and the maximum energies over particle populations in magnetospheric configuration without magnetic bubbles and in the presence of them, the time of averaged half-life of particles in the system and the maximum of ion life time in the magnetosphere. One can see from the Table that without bubbles particle acceleration is several times smaller than in the presence of bubbles. The high limit of energy is determined by the energy when ion gyroradius become large in comparison with characteristic sizes of magnetosphere and leave it. Averaged final energies of particles accelerated in magnetosphere without bubbles are about several keV (due to nonadiabatic acceleration in a neutral sheet), in the presence of bubbles they reach about several tens of keV due to scattering on bubbles, that also substantially increase the life time of ions T_{max} in the system.

Ion	$\langle E_{fin}\rangle$&E_{max}, keV				$T_{half\text{-}life}$, s		T_{max}, s	
	no bubbles		bubbles		no bub.	bub.	no bub.	bub.
	$\langle E_{fin}\rangle$	E_{max}	$\langle E_{fin}\rangle$	E_{max}				
H^+	6,5	16,8	6,4	17	28	32,5	205	217
He^+	6,9	14,5	6,6	14,3	27,3	23	274	358
O^+	6,1	14,9	5,3	13	34,5	32,9	364	506
Na^+	5,63	13,6	6	15,1	41	41,1	500	748
S^+	5,5	9,7	5,7	10,3	44	46	592	513
K^+	5,7	13,8	6,2	10,2	49,5	49	583	428

3.3. *The model of charged particles acceleration and thermalization in a turbulent plasma of a magnetotail*

Along with a global model of the Hermean magnetosphere we consider in this work the model of ion acceleration and dispersion in turbulent electromagnetic fields in plasma sheet that might appear as a result of

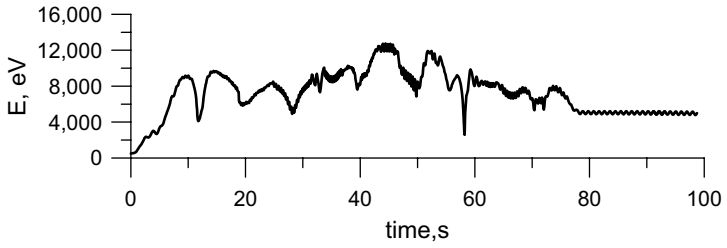

Fig. 7. The gain of energy by proton, presented in previous Fig. 6.

the development of plasma sheet instabilities. The current sheet of the magnetotail has different modes of unstable perturbations, that might develop turbulent electric and magnetic fields. Particularly, the drift modes [37], [38] are the source of plasma oscillations that propagate in a form of waves with the limited phase velocities. The different modifications of a tearing-mode [39], [40] support the local regions of the zero magnetic field B_z. Their mutual interaction and saturation lead to the development of a turbulent electromagnetic field [20], [27].

We investigated the dispersion and acceleration of ions in 1D magnetotail configuration with the turbulent field ($\delta\mathbf{B}$, $\delta\mathbf{E}$). This model is the natural generalization of the equatorial approximation, in a frame of which the mechanisms of the transport and acceleration were investigated in [41].

Let us consider the magnetic component of the turbulent field $\delta\mathbf{B}$ in the form of the wave ensemble:

$$\begin{aligned}
\delta B_x &= \textstyle\sum_{\mathbf{k}} \delta B(\mathbf{k}) \frac{k_\perp}{k} g_{\mathbf{k}}(r) \\
\delta B_y &= \textstyle\sum_{\mathbf{k}} \delta B(\mathbf{k}) \left[\frac{k_y k_x}{k_\perp k} g_{\mathbf{k}}(r) + \frac{k_z}{k_\perp} h_{\mathbf{k}}(r) \right] \\
\delta B_z &= \textstyle\sum_{\mathbf{k}} \delta B(\mathbf{k}) \left[\frac{-k_z k_x}{k_\perp k} g_{\mathbf{k}}(r) - \frac{k_y}{k_\perp} h_{\mathbf{k}}(r) \right]
\end{aligned} \tag{7}$$

Here $g_k = \cos(\mathbf{kr} + \phi_k^2 - t\omega_k)$, $h_k = \sin(\mathbf{kr} + \phi_k^1 - t\omega_k)$, $k_\perp = (k_z^2 + k_y^2)^{1/2}$. The field $\delta\mathbf{B}$ has the form that the condition $\delta\mathbf{B} = 0$ is satisfied. The initial phases ϕ_k^1 and ϕ_k^2 are the random values with a homogeneous distribution on the interval $[0, 2\pi]$. The frequency ω_k for each harmonics is chosen in such a way that the phase velocity $\omega_k/k = v_\phi$ of all waves are the same. The wave amplitude $\delta\mathbf{B}(\mathbf{k})$ is chosen accordingly to [27]. Using the system (7)

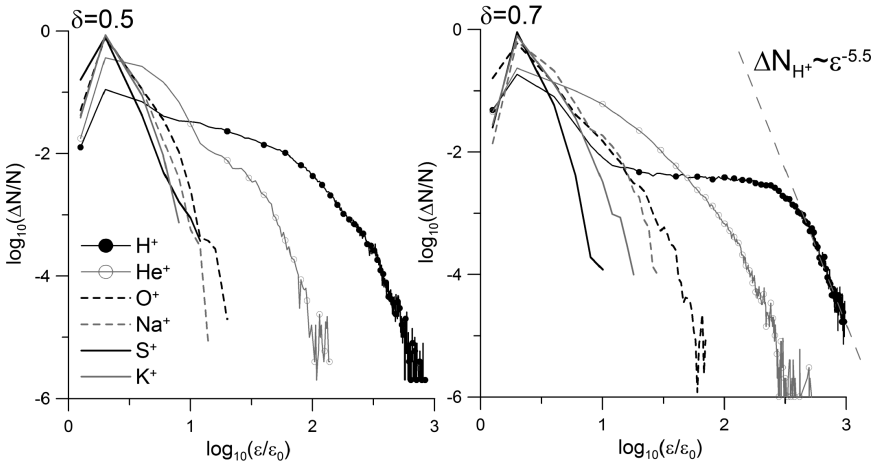

Fig. 8. Energy spectra of different kinds of ions in the system with two different levels of turbulence.

and the condition of the absence of free charges one can find the components of the electric fields from Maxwell equations.

Now let us determine the relations between the parameters of the system. The constant magnetic field is taken from the modified Harris model [36] $\mathbf{B} = B_0 \tanh(z/L)\mathbf{e}_x + B_z\mathbf{e}_z$. The value $B_z/B_0 = 0.1$ is taken for calculation. We use dimensionless magnitude of turbulent magnetic field $\delta = \langle \delta\mathbf{B}^2 \rangle^{1/2}/B_0$.

The ions are traced from the upper and down limits of the current sheet. The initial distribution function on energies is taken as Maxwellian distribution with temperature $mv_0^2/2$. To calculate the averaged gain of energy of ions we use the following scheme. The time of modeling is limited by the time when all particles escape from the current sheet. After collection of particle parameters at the boundaries of the modeling region one can obtain the corresponding energy spectra of particles. The examples of these spectra at several values of parameter δ and several kinds of ions are presented in figure 8. One can see that in all cases of interaction of protons with a turbulent electromagnetic field the "tail" of energetic distribution appears. Generally the new distribution of protons at high energies has a power dependence $f \sim \varepsilon^{-\kappa}$ (the corresponding values of κ are also shown in figure). Therefore the group of protons with energies $\varepsilon \sim (10^2 - 10^3)\varepsilon_0$ appears in the system. The analogous results are obtained for He^+ ions. The oxygen ions form a power spectra at quite strong level of turbulence.

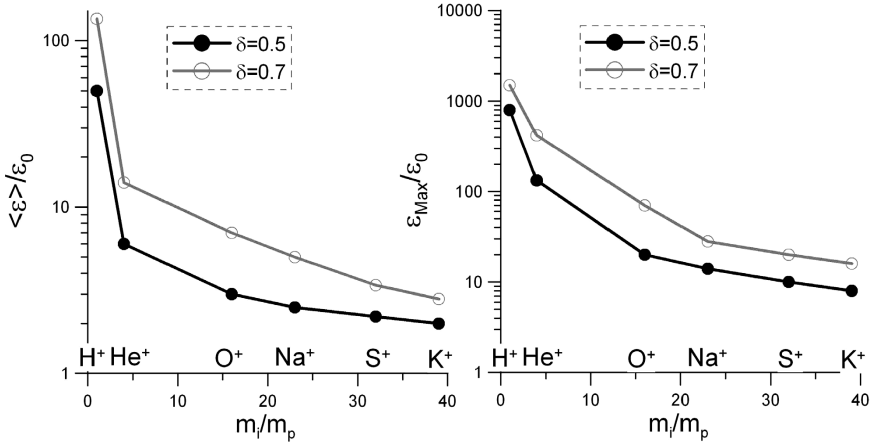

Fig. 9. The values of an average and maximum energy for different kinds of ions.

More heavy ions also increase an average energy $\langle\varepsilon\rangle$, but the power spectra is not formed.

The effect of the growth of average ion energy is presented in Figure 9. In this figure one can see also the values of maximum ion energy that are generalized in the Table 5. Taking into account the amplitude of the magnetic field of current sheet $B_0 \sim 20\,\mathrm{nT}$ and its thickness in proton gyroradius, one can receive the value $\varepsilon_0 \sim 1-5\,\mathrm{keV}$. Generally one can say that the mechanism of ion thermalization by the turbulent electromagnetic field is more effective for p^+ and He^+ ions than the mechanism of multiple dipolarization (their maximum energies are correspondingly $\sim$1500 keV and $\sim$420 keV). For heavier ions as O^+ the mechanism of a turbulent acceleration is not so effective as ones presented in the Table 5.

The mechanism of a "turbulent" acceleration has limits due to limited space parameters of the system. Thus the cross-tail distance of current sheet of Mercury is about $\sim 10^4$ km. At the same time this mechanism is the most effective if the scale of particle gyroradius in the center (where $|\mathbf{B}_0| \sim 10-5\,\mathrm{nT}$) were less or about the Larmor gyroradius in the center of current sheet where protons with energies 10^2 keV will have Larmor radius about $\sim 10^4$ km. The despite the potential possibility to be accelerated to 1 MεB, plasma protons might be accelerated only to 200 keV in the Hermean magnetosphere. For another kind of more heavier particles the gain of energy will be lesser (the Larmor radius is proportional the root square from the mass). For example, ions K^+ with energies about 30 keV escape

from the magnetosphere because their Larmor radius is larger than the scale of current sheet.

	The maximum of obtained energy at $\delta = 0.7$
p	1500 KeV
He^+	140 KeV
O^+	70 KeV
Na^+	30 KeV
S^+	20 KeV
K^+	16 KeV

4. Conclusions

Small scales of plasma processes in the Hermean magnetosphere in comparison with the Earth's one are the reason of some difference between the mechanisms of particle accelerations in their magnetotails. The role of nonadiabatic effects of particle motion near Mercury is expected to be more pronounced in comparison with the Earth. Our numerical calculations demonstrated that the contribution of nonadiabatic acceleration across current sheet and particle heating due to scattering on moving magnetic bubbles might give similar contributions (energy gain about several tens keV) to the energy distributions of plasma in the magnetotail of Mercury. The mechanism of multiple substorm dipolarizations in Mercury magnetosphere might be more effective than in the Earth's one due to more high substorm activity in the Hermean magnetosphere. Particle acceleration to high energies is effective during the first 1-2 substorm cycles, after this the particles go out from the magnetosphere. Heavy particles as O^+, Na^+, S^+, K^+ might be accelerated during several cycles of dipolarization, acquiring the final energies about several tens of keV. Generally this mechanism plasma acceleration might favorize the observation of ions with limiting energies $\sim$100 keV and hot electrons with energies $\sim$200 keV at distances about $\sim R_M$ in the magnetotail.

Mechanisms of particle scattering on electric and magnetic waves can play an important role in both ions and electrons heating. We estimated electron energies in Mercury magnetosphere up to 300 keV. Because magnetic field of Mercury is weaker than the Earth's one should expect that for Mercury the role of fluctuations will be large contrary to the Earth where their role is significant in the region down stream from the

distant X-line. Our estimates demonstrate that the turbulence in current sheet can increase the averaged energy of protons approximately in 10^2-10^4 times.

Generally, the combination of both these mechanisms of particle acceleration that might be realized under different conditions in the Hermean magnetosphere might support particle heating with an upper limit about several hundreds keV, that is smaller than in the Earth due to small size of the Hermean magnetosphere. The particles with higher energies might not be trapped inside the last one; the most part of them escape to the solar wind.

References

1. N.F. Ness, Behannon K.W., Lepping R.P., *Nature*, **255**, (1975) 204.
2. J.A. Slavin, Acuna M.H., Anderson B.J. *et al.*, *Science*, **321**, (2008) 85.
3. D.C. Delcourt, Saito Y., Illiano J.M. *et al.*, *Adv. Space Res.*, **43**, (2009) 869.
4. T. Armstrong, Krimigis S., Lanzerotti L., *J. Geophys. Res.*, **80**, (1975) 4015.
5. J.H. Eraker, J.A. Simpson, *J.Geophys. Res.*, **91**, (1986) 9973.
6. J.A. Slavin, Acuna M.H., Anderson B.J. *et al.*, *Science*, **324**, (2009) 606.
7. G.L. Siscoe, Ness N. F., Yeates C. M., *J.Geophys.Res.*, **80**, (1975) 4359.
8. S.P. Christon, *Icarus*, **71**, (1987) 448.
9. W.-H. Ip, *Icarus*, **71**, (1987) 441.
10. J. Büchner, L.M. Zelenyi, *J. Geophys. Res.*, **94**, (1989) 11821.
11. J.A. Simpson, J.H. Eraker, J.E. Lamport *et al.*, *Science*, **185**, (1974) 160.
12. E. Kirsh, Richter A.K., *Ann. Geophys.*, **3**, (1985) 13.
13. S.P. Christon, Daly S.F., Eraker J. *et al.*, *J. Geophys. Res.*, **84**, (1979) 4277.
14. L.M. Zelenyi, Lominadze J., Taktakishvili A., *J. Geophys. Res.*, **95**, (1990) 3883.
15. W.-H. Ip, *Adv. Space Res.*, **19**, (1997) 1615.
16. T. H. Zurbuchen, Raines J.M., Gloeckler G. *et al.*, *40th Lunar and Planetary Science Conference*, (2009), id. 2141.
17. M. Sarantos, Slavin J.A., Benna M. *et al.*, *Geophys. Res. Let.*, **36**, (2009) L04106.
18. L.M. Zelenyi, Oka M., Malova H.V. *et al.*, *Sp. Sci. Rev.*, **132**, (2007) 593.
19. D.C. Delcourt, K. Seki, N. Terada *et al.*, *Ann. Geophys.*, **23**, (2005) 3389.
20. L.M. Zelenyi, Milovanov A.V., *Uspehi.* 174, (2004) 809.
21. D.C. Delcourt and Martin R.F., *J. Geophys. Res.*, **99**, (1994) 23583.
22. K.-H. Glassmeier, N. Mager, D. Klimushkin, *Geophys. Res. Lett.*, **30**, (2003) 1928.
23. Baumjohann W., Matsuoka A., Glassmeier K.-H. *et al.*, Adv. Space Res., **38**, (2006) 604.
24. D.C. Delcourt, *J. Atmosp. Sol.-Terr. Phys.*, **64**, (2002) 551.
25. E. Fermi, *Phys. Rev.*, **75**, (1949) 1169.
26. M. Hoshino, Nishida A., *et al.*, *Geophys. Res. Lett.*, **21**, (1994) 2935.

27. P. Veltri, Zimbardo G., *et al.*, *J. Geophys. Res.*, **103**, (1998) 14897.
28. L.R. Lyons, Speiser T.W., *J. Geophys. Res.*, **87**, (1982) 2276.
29. M. Ashour-Abdalla, Berchem J.P., Buechner J. *et al.*, *Geophys. Res. Lett.*, **17**, (1990) 2317.
30. M. Ashour-Abdalla, Berchem J.P., Buechner J. *et al.*, *J. Geophys. Res.*, **98**, (1993) 5651.
31. T.W. Speiser, *J. Geophys. Res.*, **70**, (1965) 1717.
32. D.N. Baker, Borovsky J., Burns J. *et al.*, *J. Geophys. Res.*, **92**, (1987) 4707.
33. W.W. Liu, Rostoker G., *J.Geophys. Res.*, **100**, (1995) 21897.
34. J.G. Luhmann, Friesen L.M., *J. Geophys. Res.*, **84**, (1979) 4405.
35. S. Perri, Lepreti F., Carbone V. *et al.*, *Europhys. Lett.*, **78**, (2007) 40003.
36. E.G. Harris, *Nuovo Chimento*, **23**, (1962) 115.
37. W. Daughton, *Phys. Plasmas*, **6**, (1999) 1329.
38. L.M. Zelenyi, Artemyev A.V., Petrukovich A.A. *et al.*, *Ann.Geophys.*, 27, (2009) 861.
39. B. Coppi, Laval G., Pellat R., *Phys. Rev. Lett.*, **16**, (1966) 1207.
40. L. M. Zelenyi, Artemyev A.V., Malova H.V. *et al.*, *J. Atmosp. Sol.-Terr. Phys.*, **70**, (2008) 325.
41. L.M. Zelenyi, Artemyev A.V., Malova .V. *et al.*, *Phys. Lett. A*, **372**, (2008) 6284.